Amplified spontaneous emission spectrum and gain characteristic of a two-electrode semiconductor optical amplifier*

Wang Hanchao(汪寒超), Huang Lirong(黄黎蓉)†, and Shi Zhongwei(石忠卫)

Wuhan National Laboratory for Optoelectronics, College of Opto-Electronics Science & Engineering, Huazhong University of Science & Technology, Wuhan 430074, China

Abstract: A two-electrode multi-quantum-well semiconductor optical amplifier is designed and fabricated. The amplified spontaneous emission (ASE) spectrum and gain were measured and analyzed. It is shown that the ASE spectrum and gain characteristic are greatly influenced by the distribution of the injection current density. By changing the injection current density of two electrodes, the full width at half maximum, peak wavelength, peak power of the ASE spectrum and the gain characteristic can be easily controlled.

Key words: semiconductor optical amplifier (SOA); current density; amplified spontaneous emission (ASE); gain characteristic

DOI: 10.1088/1674-4926/32/6/064010 **PACC:** 4280S; 6855; 4285F

1. Introduction

Semiconductor optical amplifiers (SOAs) have been widely used as inline amplifiers, wavelength converters and optical regeneration devices in optical communication systems. In these linear or nonlinear applications, the gain spectrum is an important parameter that characterizes a SOA. Wideband optical communication requires optical amplifiers with a broad spectral emission and a high gain characteristic. As an amplified spontaneous emission (ASE) spectrum is similar to that of small signal gain (SSG) spectrum when the SSG of an SOA is large enough, the ASE spectrum can be used to evaluate the SSG spectra to some extent[1]. This makes the study of the spectral emission characteristics of SOAs important.

A multi-electrode method has been used for optical bistability in laser diodes[2] and for broad bandwidths in semiconductor super-luminescent diodes[3]. In recent years, multi-electrode SOAs have theoretically demonstrated their potential advantages for various applications. For example, they can improve a small-signal modulation bandwidth[4] and enhance the reception response and bandwidth of a photo detector[5]. We have proposed a two-electrode SOA for improving steady state and dynamic performance, and theoretically proved that it can manipulate the frequency chirp[6], control the gain spectrum and increase saturation output power[7, 8], enhance gain recovery rate and cross-gain modulation bandwidth[9], and reduce the pattern effects in wavelength conversion[10]. However, there have been no reports on controlling the ASE spectrum and gain characteristic of a two-electrode SOA by adjusting the injection current density of the two electrodes.

In this paper, we design and fabricate a two-electrode multi-quantum well (MQW) SOA and investigate the ASE spectrum and gain characteristic at different current density distributions. We find that the ASE spectrum and gain characteristic of a two-electrode SOA can be easily controlled by adjusting the injection current density of the two electrodes.

2. Device structure and experimental detail

Unlike a common SOA, as shown in Fig. 1(a), which has only one electrode and a uniform distribution of injection current density along the cavity, the two-electrode MQW SOA we fabricated consists of two electrodes and two sections separated by a narrow SiO_2 isolating channel, as shown in Fig. 1(b).

The material epitaxy of the SOA was performed by metal-organic chemical vapor deposition (MOCVD) on an n-InP substrate. The active region consisted of 3 tensile-strain InGaAsP wells and 4 compressively strained InGaAsP wells in order to make the gain polarization insensitive. The SOA is of a ridge waveguide structure with its width W being 2 μm and its total length L being 1200 μm. An insulating channel was fabricated by wet-etching and plasma-enhanced chemical vapour deposition of SiO_2 film; as a result, the SOA was divided into two electrodes and two sections, one section had a length of L_1, being 826 μm, the other section had a length of L_2, being 354 μm, and the insulating channel length was about 20 μm. Owing to the insulating channel, the two electrodes are electrically isolated and the bias currents are I_1 and I_2, respectively. The corresponding current densities of the two sections, J_1 and J_2, are expressed as $J_1 = I_1/WL_1$, $J_2 = I_2/WL_2$. The facets were anti-reflectively coated to minimize reflectivity; and the stripe was tilted at 7° from the facet to further reduce residual reflectivity. The facet near the section with length L_1 is referred to as facet 1, while the other facet, near the section with length L_2, is referred to as facet 2.

We measured the ASE spectra and gain of the two-electrode SOA as a function of I_1. Figure 2 shows the experimental setup for ASE and gain characteristic measurements. The ASE measurements were performed by a Yokogama

* Project supported by the National High Technology Research and Development Program of China (No. 2007AA03Z414) and the National Natural Science Foundation of China (No. 60777019).

† Corresponding author. Email: hlr5649@163.com

Received 28 December 2010, revised manuscript received 23 February 2011

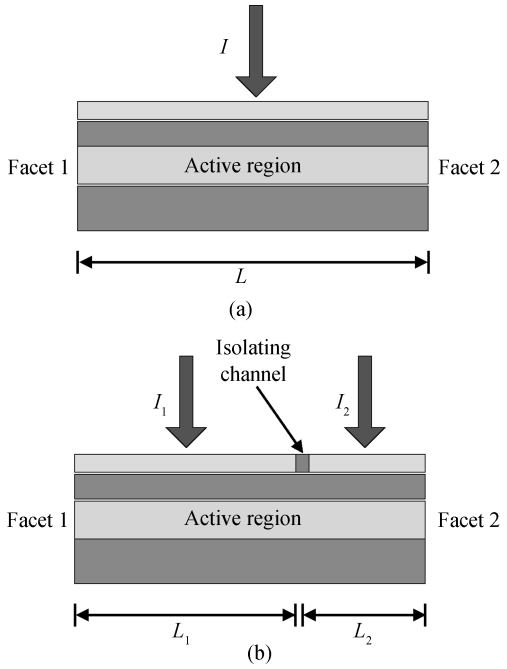

Fig. 1. Basic structures of (a) a common SOA and (b) a two-electrode SOA.

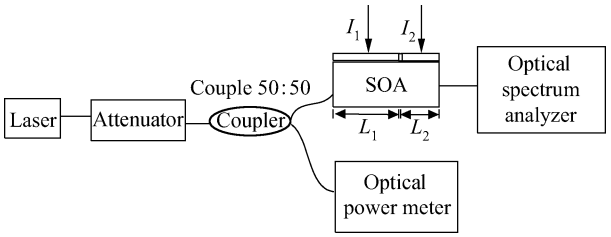

Fig. 2. Experimental setup for the ASE spectrum and gain measurement of the SOA.

AQ6370 optical spectrum analyzer. For gain measurement, the output power of the laser was divided into two branches by a 3-dB coupler following the optical attenuator. The input optical power was measured by an optical power meter and the output signal from the SOA was measured by the optical spectrum analyzer.

3. Results and discussion

3.1. ASE spectrum characteristics

The ASE spectrum output from facet 2 at different injection current distributions are plotted in Fig. 3. For all the spectra, the total injection current ($I = I_1 + I_2$) is fixed at 350 mA. The ASE spectra have very small ripples with a wide range of wavelengths; this is due to the optimal antireflective coating and the 7° tilted waveguide[11].

To further analyze the ASE spectra, we investigate the full width at half maximum (FWHM), peak wavelength and peak power from different output facets, and the total injection current is fixed at 300 mA and 350 mA, respectively. We find that the FWHM variation trends, peak wavelength and peak power are similar for both cases. For the sake of simplicity, we will

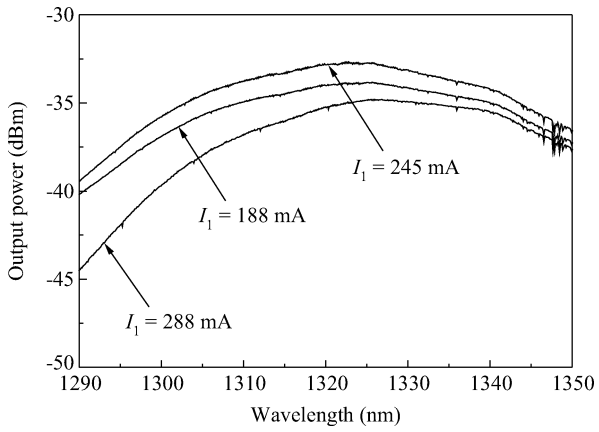

Fig. 3. ASE spectrum output from facet 1 with different I_1.

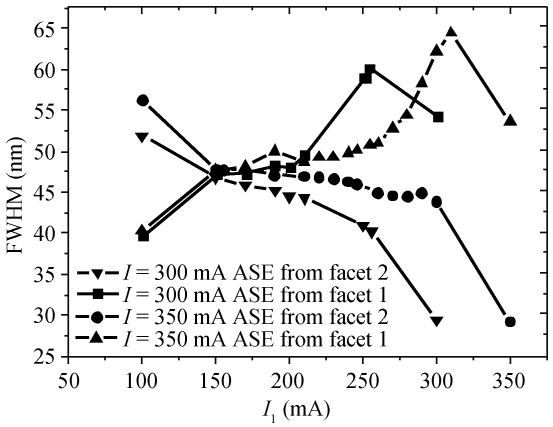

Fig. 4. FWHM of ASE spectra versus I_1.

only discuss the case of the injection current fixed at 350 mA in the following. Figure 4 shows the FWHM of the ASE spectra versus I_1. The FWHM of the ASE spectrum from facet 1 firstly broadens and then decreases as I_1 increases; in contrast, the FWHM of the ASE spectrum from facet 2 narrows with I_1. It is noted that, in the latter case, the decrease of I_1 results in an increase of I_2 injected at the output electrode. As the injection current at the output electrode increases, due to the band-filling effect, the range of carrier distribution in the energy level becomes wider and the spectrum width then increases. Therefore, the higher the current density of output electrode, the wider the FWHM of the ASE spectrum from the SOA output facet. However, as the current density injected at the output electrode becomes too large, owing to a thermal effect in the output electrode, the spectrum width decreases instead.

Figure 5 shows the peak wavelength of the ASE spectra versus I_1. When I_1 is not very high, the peak wavelengths of the ASE spectrum output from facets 1 and 2 are about the same. However, as I_1 increases, the carrier density of the ASE spectrum output from facet 1 increases, and then the peak wavelength of the ASE spectrum blue-shifts as a result of the band-filling effect.

In contrast, for the ASE spectrum output from facet 2, the peak wavelength firstly decreases and then increases with the increase of I_1. The first peak wavelength decrease is due to the thermal effect in section L_2. When I_1 is much smaller than

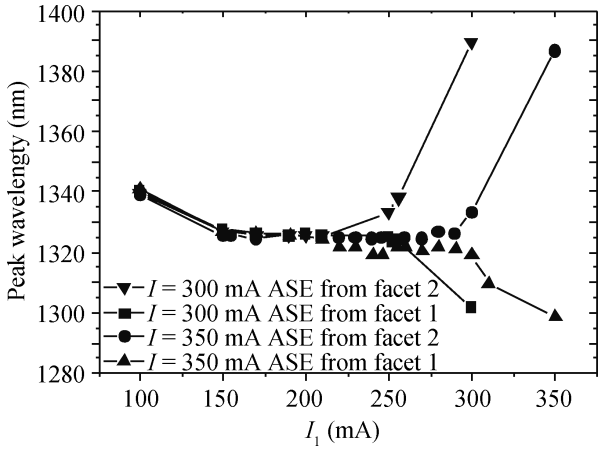

Fig. 5. Peak wavelength of ASE spectra versus I_1.

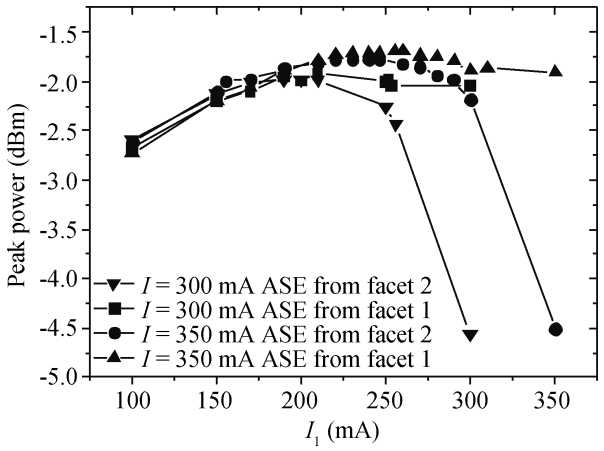

Fig. 6. Peak power of the ASE spectra as a function of I_1.

150 mA, the current density injected into section L_2 is excessively high, which produces a significant thermal effect and narrows the energy band gap. Therefore, the peak wavelength at the beginning is larger. With the increase of I_1, the increase of J_1 in combination with the decrease of J_2 causes the thermal effect in section L_2 to gradually reduce. As a result, the band gap broadens and then the peak wavelength of the ASE spectrum output from facet 2 decreases correspondingly. As I_1 further increases to over 250 mA, the band-filling effect plays a leading role.

Figure 6 shows the peak power variation of the ASE spectra versus I_1. The peak powers of the ASE spectrum output from facets 1 and 2 have a similar dependence on I_1. The peak power increases first, and reaches to a maximum at about 245 mA and then drops down. Theoretically, the SOA can be divided into many small sub-segments and the peak power of the SOA is proportional to the product of modal gain of every sub-segment[12]. The larger the modal gain difference among the sub-segments, the smaller peak power the SOA obtains. Because of the non-uniform current density distribution along the direction of optical propagation, the peak power of the two-electrode SOA is thus smaller than that of a common SOA in which $I_1 = 245$ mA.

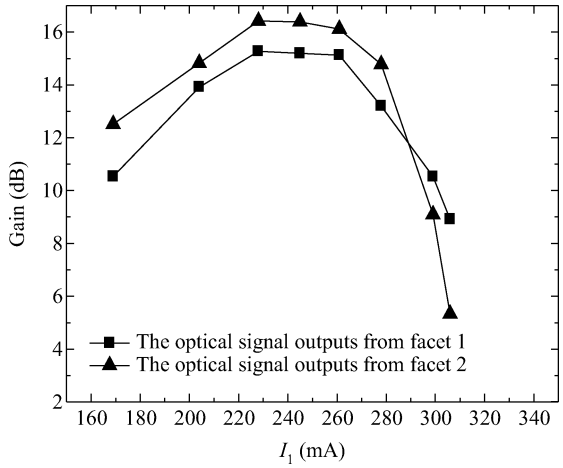

Fig. 7. Fiber-to-fiber gain as a function of I_1.

3.2. Gain characteristic

Figure 7 shows the small signal fiber-to-fiber gain versus I_1 for an input signal of –25 dBm at 1309 nm. The total injection current is 350 mA. We study two further cases. In the first case, the optical signal inputs into facet 1 and outputs from facet 2; while in the second case, the optical signal enters facet 2 and outputs from the back facet 1.

As shown in Fig. 7, the gains in the two cases have roughly the same variation tendency as the peak power of ASE spectra shown in Fig. 6. When I_1 increases, the gain increases firstly, with its value reaches to a maximum when I_1 is about 245 mA, and then it drops down, which is due to the same reason as the peak power variation of ASE spectra in Fig. 6. When I_1 equals to 245 mA, the injection current density ratio is $J_1 : J_2 = 1.0$. At this time, the two-electrode SOA is equivalent to a common SOA, the distribution of current density is uniform along the direction of optical propagation and then the product of the modal gain of every sub-segment is at its biggest. This indicates that the common SOA has a higher signal fiber-to-fiber gain than a two-electrode SOA.

4. Conclusions

In conclusion, we have designed and fabricated a two-electrode QW-SOA. Compared to a common SOA, a two-electrode QW-SOA can be adjusted flexibly to obtain a non-uniform current density distribution. It is indicated that ASE spectra and gain are greatly influenced by current density distribution and the output facet of a two-electrode SOA. By changing the injection current density of the two electrodes, the FWHM, peak wavelength, peak power of ASE spectrum and fiber-to-fiber gain can be easily controlled.

References

[1] Miao Q Y, Huang D X, Liu D M, et al. Rapid evaluation of gain spectra from measured ASE spectra of travelling-wave semiconductor optical amplifier. Chinese Optics Letters, 2004, 8: 483

[2] Kawaguchi H. Absorptive and dispersive bistability in semiconductor injection lasers. Opt Quantum Electron, 1992, 19: s1

[3] Xin Y C, Martinez A, Saiz T, et al. 1.3 μm quantum-dot multi-

section superlumiescent diodes with extremely broad bandwidth. IEEE Photonics Technol Lett, 2007, 19(7): 501

[4] Kim H S, Choi B S, Kim K S, et al. Improvement of modulation bandwidth in multisection RSOA for colorless WDM-PON. Opt Express, 2009, 17(19): 16372

[5] Sharaiha A, Guegan M. Equivalent circuit model for multi-electrode semiconductor optical amplifiers and analysis of inline photodetection in bidirectional transmissions. J Lightwave Technol, 2000, 18(5): 700

[6] Tian P, Huang L R, Yan L J, et al. Chirp characteristics of wavelength converter in multi-electrode semiconductor optical amplifiers. Proc SPIE, 2008, 7279: 727919

[7] Huang L R, Yu S H, Huang D X. Gain spectrum and saturation characteristics of two-segment semiconductor optical amplifier. Proc SPIE, 2008, 7135: 71352C

[8] Zhu S S, Huang L R, Chen Y. Gain spectrum control in multi-Electrode semiconductor optical amplifiers. Proc SPIE, 2008, 7278: 72781V

[9] Yu Y, Huang L R, Xiong M, et al. Enhancement of gain recovery rate and cross-gain modulation bandwidth using a two-electrode quantum-dot semiconductor optical amplifier. Journal of the Optical Society of America B, 2010, 27(11): 2211

[10] Tian P, Huang L R, Hong W, et al. Pattern effect reduction in all-optical wavelength conversion using a two-electrode semiconductor optical amplifier. Appl Opt, 2010, 49(26): 5005

[11] Huang L R, Huang D X, Zhang X L. Optimal design of antireflection coating for flat and wideband incoherent optical source based on semiconductor optical amplifier. Chinese Journal of Semiconductors, 2006, 27(8): 1471

[12] Connelly M J. Wideband semiconductor optical amplifier steady-state numerical model. IEEE J Quantum Electron, 2001, 37(3): 439